

University of Louisville

## ThinkIR: The University of Louisville's Institutional Repository

---

College of Arts & Sciences Senior Honors  
Theses

College of Arts & Sciences


---

5-2021

### Oriented external electric field (OEEF) tuning of unsubstituted azoheteroarene photoswitching performance.

Irma Avdic  
*University of Louisville*

Follow this and additional works at: <https://ir.library.louisville.edu/honors>

 Part of the [Other Chemistry Commons](#)

---

#### Recommended Citation

Avdic, Irma, "Oriented external electric field (OEEF) tuning of unsubstituted azoheteroarene photoswitching performance." (2021). *College of Arts & Sciences Senior Honors Theses*. Paper 257. Retrieved from <https://ir.library.louisville.edu/honors/257>

This Senior Honors Thesis is brought to you for free and open access by the College of Arts & Sciences at ThinkIR: The University of Louisville's Institutional Repository. It has been accepted for inclusion in College of Arts & Sciences Senior Honors Theses by an authorized administrator of ThinkIR: The University of Louisville's Institutional Repository. This title appears here courtesy of the author, who has retained all other copyrights. For more information, please contact [thinkir@louisville.edu](mailto:thinkir@louisville.edu).

Oriented external electric field (OEEF) tuning of unsubstituted azoheteroarene photoswitching  
performance

By

Irma Avdic

Submitted in partial fulfillment of the requirements

for Graduation *summa cum laude*

and

for Graduation with Honors from the Department of Chemistry

University of Louisville

May, 2021

## **ACKNOWLEDGEMENTS**

I would like to thank the following people, without whom I would not have been able to complete this research, and without whom my last year of undergraduate studies would not have been this successful! First, I would like to express my deepest gratitude to my supervisor, Dr. Lee Thompson, whose support and guidance helped me develop technical and conceptual skills that brought my work to a higher level. In addition, I would like to thank my defense committee members, Dr. Frederick Luzzio and Dr. Cynthia Corbitt, for their time and intellectual contributions to this project. I would also like to thank Emily Kempfer-Robertson for her mentorship, encouragement, and friendship during the last year of my undergraduate research career. Thank you, Emily for always patiently answering my questions and for training me to think outside of the box. Thank you to the entire Thompson research group for helping me improve my listening and presentation skills and for helping me learn something new during every one of our meetings. Thank you to my current, and past professors, for challenging me and helping me build passion and enthusiasm for the subject. Finally, to my parents, my brother, and my partner for all your patience, love, and support – thank you!

## TABLE OF CONTENTS

List of Tables .....	4
List of Figures .....	5
Abstract .....	6
Introduction .....	7
Theory .....	9
Computational Details and Methodology .....	13
Results and Discussion	
Gibbs Reaction Energies .....	16
Dipoles and First Hyperpolarizabilities .....	22
Gibbs Activation Energies and Thermal Half-Lives .....	25
Wiberg Indices .....	29
Conclusions .....	33
References .....	34

## LIST OF TABLES

Table 1 - Comparison of the performance of various functionals benchmarked on the field-free im type I structure.....	14
Table 2 - Total first hyperpolarizabilities calculated for E and Z isomers and inv TS of the studied molecules in the field-free environment, along with NN and NC bond lengths of inv TS .....	22
Table 3 - Thermal half-lives calculated for the studied molecules in the field-free environment as compared to the experimental half-lives calculated for the methylated derivatives. ...	25
Table 4 - Thermal half-lives reported in days for all molecules under the application of $F_{\text{azo}}$ . ...	27
Table 5 - Thermal half-lives reported in days for all molecules under the application of $F_{\text{het}}$ .....	28
Table 6 - Highest thermal half-lives calculated for the studied molecules in the field environment along with the NN and NC bond lengths of their inv TSs and their respective WIs ...	30

## LIST OF FIGURES

Figure 1 – Optimized $S_0$ E isomers of im (a), pz (b), and py (c) .....	6
Figure 2 - Comparison of the performance of various functionals benchmarked on the im type I structure in the field environment. ....	14
Figure 3 - OEEF directions demonstrated on the $S_0$ E isomer of azopyrrole.....	15
Figure 4 - Optimized $S_0$ E isomers of all studied molecules .....	16
Figure 5 - Optimized structures of azoimidazole type I $S_0$ stationary points showing both $S_0$ rotation and inversion pathways. ....	17
Figure 6 - Optimized $S_0$ Z isomer of im type I in the T-shaped conformation. ....	17
Figure 7 - Reaction Gibbs energy for the $S_0$ Z isomer of im as a function of field strength .....	19
Figure 8 - Reaction Gibbs energy for the $S_0$ Z isomer of pz as a function of field strength .....	20
Figure 9 - Reaction Gibbs energy for the $S_0$ Z isomer of py as a function of field strength .....	20
Figure 10 - Optimized $S_0$ inv TS of im type II showing the N14=C5 bond .....	23
Figure 11 - Total first hyperpolarizability as a function of field strength .....	24
Figure 12 - Optimized $S_0$ Z isomer of all studied molecules. ....	31

## ABSTRACT

Azoheteroarenes are relatively new photoswitchable compounds, where one of the phenyl rings of an azobenzene molecule is replaced by a heteroaromatic five-membered ring. Although few studies have been performed, recent findings on methylated azoheteroarenes show that these photoswitches have great potential in various optically addressable applications. Thermal stability of molecular switches is one of the primary factors considered in the design process. For the purposes of quick information transmission in materials science, the thermal (Z – E) relaxation process should be as short as possible. On the other hand, molecular memory storage devices prefer long Z - E relaxation times. In this computational study, we investigate how oriented external electric fields (OEEFs) can be used to tune the photoswitching properties of three unsubstituted heteroaryl azo compounds – azoimidazole (**im**), azopyrazole (**pz**), and azopyrrole (**py**). (Figure 1) Based on a density functional theory (DFT) approach, we examine the electric field control of the thermal half-lives and nonlinear optical properties of **im**, **pz**, and **py**. We show that favorable OEEF orientations can increase thermal half-life of studied molecules by as much as 60 times, compared to their half-life values in the field-free environment. A deeper understanding of the kinetic and nonlinear optical properties provides greater insight of how molecular switches can be enhanced for user-selective design in different environments.

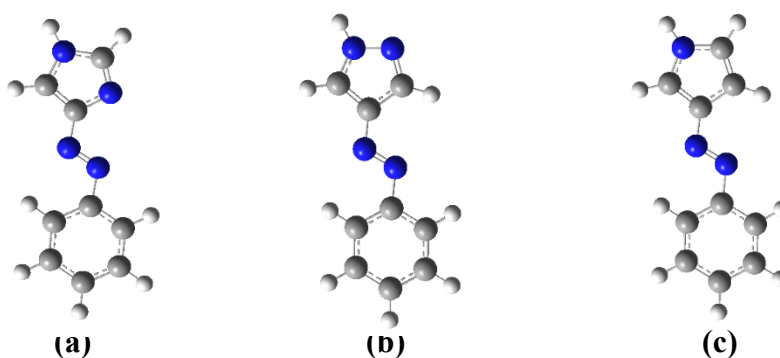


**Figure 1.** Ground state ( $S_0$ ) optimized E isomers of **im** (a), **pz** (b), and **py** (c). Color assignments: gray – C atom, white – H atom, blue – N atom.

## INTRODUCTION

Molecular switches are molecular systems that can reversibly shift between at least two different states.<sup>1</sup> Azobenzene (AB) has been studied extensively as a prototypical photoswitch molecule<sup>2-5,21</sup> and its applications range from memory devices<sup>6,7</sup> to molecular motors and actuators.<sup>8-10</sup> AB exhibits a photo-induced isomerization process, converting from its E (*trans*) isomer to Z (*cis*) isomer, after which a thermal relaxation back to the E isomer can occur. Thermal stability of a photoswitch represents one of the important properties of the photoswitch performance. Another factor that influences the switch's potential is the completeness of the photoswitching process.<sup>11</sup> Certain drawbacks of AB, such as its incomplete photoswitching due to overlapping absorbance of the two isomers<sup>12</sup>, have confirmed the need for modified molecular switches.

In recent years, azoheteroarenes, a new class of AB-based photoswitches, have been synthesized and found to provide more efficient and suitable molecular switches for a variety of uses.<sup>11,16,17</sup> Azoheteroarenes are compounds having one or both rings of AB substituted by a five-membered heteroaromatic ring (usually nitrogen-based). These compounds provide long thermal half-life of the Z isomer and substantial quantitative switching to the E isomer.<sup>13</sup> To the best of our knowledge, most research regarding these compounds has focused on the effect of methylation, of one or both rings, on the photoswitching response.<sup>11,13-15</sup> Due to the electron-donating character of the methyl group, such switches provide longer thermal relaxation times. In contrast, few studies have been performed regarding heteroarenes that lack methyl groups on the heterocyclic ring, and how they can be improved to offer better switching performance.

Previous work done by Calbo and co-workers reports a list of novel azoheteroarene photoswitches with Z isomer half-lives ranging from seconds to years, all through tuning of the



heteroaromatic ring.<sup>11</sup> The highest performing molecular switches from the groups of pyrazole, imidazole, and pyrrole molecules are studied in this work (figure 1). All three molecular representatives are studied without the additional methyl groups on the heterocyclic ring, i.e., the unsubstituted equivalents are considered. The motivation for studying unsubstituted azoheteroarenes comes from the lack of additional steric hindrance of these compounds caused by methylation, making them particularly useful in photopharmacology<sup>16,24</sup>, as part of a drug delivery system, and as potential photoswitches for biomolecules.<sup>17</sup> Moreover, these compounds can be synthesized inexpensively and do not require an additional methylation step in the synthesis process.<sup>32</sup>

Based on a recent study of the photo and thermal isomerization of AB<sup>23</sup>, oriented external electric fields (OEEFs) have been demonstrated as a highly feasible design route for molecular devices. In this work, we describe how OEEFs alter the thermal behavior of unsubstituted azoheteroarenes. Specifically, we computationally explore how the electric fields control partial and complete conjugation of specific azoheteroarenes, and how this field-induced repolarization affects their relaxation time and nonlinear optical properties. Due to their strong dipole character and promising photoswitching potential, azoimidazole (**im**), azopyrazole (**pz**), and azopyrrole (**py**) were classified as the appropriate candidates for the OEEF application. Electric field gradients have, and are still being used as a research tool to control chemical reactions via manipulation of activation energy barriers through stabilization of valence bond structures.<sup>25,26,27</sup> OEEFs can modify the orientation of molecules and the overall  $\pi$  conjugation of conjugated systems. The distortion in electronic distributions and nuclear positions of a polar molecule, caused by OEEFs of adequate magnitude, can temporarily be used to manipulate the preferred isomerization pathway of a photochemical reaction.

To assess the tuning effects of the applied OEEFs, we consider kinetic properties of the studied molecules. Thermal stability of potential molecular switches is one of the primary factors considered in the photoswitch design process. For the purposes of quick information transmission in materials science, the Z - E relaxation process should be as short as possible.<sup>26</sup> On the other hand, molecular memory storage devices prefer long Z - E relaxation times.<sup>6,7</sup> Here, we use the Wiberg Index (WI) method to explain the correlation between the calculated thermal half-lives and the OEEF effects on the length of the Z - E isomerization of **im**, **pz**, and **py**. In addition, we elucidate trends in the ground state first hyperpolarizabilities of these molecules as an assessment of the nonlinear optical properties that would contribute to the switch design.

## **THEORY**

Electric dipole moment ( $\mu$ ) is the first nonzero term in a multipole expansion of charge distribution in a neutral molecule.  $\mu$  is a vector that has three components,  $\mu_x$ ,  $\mu_y$ , and  $\mu_z$ , corresponding to the directions in which the dipole contributions from atoms (or molecules) of a system lie. The direction of  $\mu$  represents the dipole orientation while the length of  $\mu$  represents its magnitude. Total dipole moment is related to its vector components as follows,

$$\mu_{total} = (\mu_x^2 + \mu_y^2 + \mu_z^2)^{1/2}.$$

Fundamentally, a dipole moment is the product of charge (C, coulomb) and length (m, meter), so the SI unit of  $\mu$  is C m. However, it is common practice in chemistry to express the total dipole moment in debye, D, where  $1 \text{ D} = 3.33564 \times 10^{-30} \text{ C m}$ . Any reported  $\mu$  values will, therefore, be expressed in debye in this work. In the presence of an electric field, the permanent dipole moment reorients to follow the field, i.e., the molecule rotates into a new direction. For example, AB

molecules can be attached to immobile media, so that the electric fields can be applied with respect to a fixed orientation of the molecule.<sup>38</sup>

In this work, we compare total dipole moments of different structures of **im**, **pz**, and **py**, and study how the electric field direction affects the dipole moment magnitude of the three azoheteroarenes. The electric field sign convention is the same as that used by Shaik and co-workers, where the positive sign indicates that the field gradient along the specified axis points from the negative charge to the positive charge.<sup>18</sup>

Aside from creating a difference in a system's dipole magnitude and direction, electric fields can also change optical properties of that system, giving rise to nonlinear optical phenomena. At low light intensity, most systems respond linearly, given by

$$\mu = \alpha E,$$

where  $\alpha$  is the polarizability and  $E$  is the incident electric field. The nonlinear response of a system can be written as a Taylor series expansion,

$$\mu = \alpha E + \frac{1}{2}\beta E^2 + \frac{1}{6}\gamma E^3 \dots, \quad (1)$$

where  $\beta$  is the first hyperpolarizability and  $\gamma$  is the second hyperpolarizability of the system. From equation (1), it can be seen that at low field magnitudes, polarization approximates a linear response, whereas with increasing field strength, nonlinear properties become more important. Similar to the total dipole calculation, total first hyperpolarizability can be calculated as follows,

$$\beta = (\beta_x^2 + \beta_y^2 + \beta_z^2)^{1/2}.$$

However, this relationship is quite oversimplified, neglecting the tensorial nature of the system's ability to polarize, i.e., the system's second-order electric susceptibility per unit volume.<sup>28</sup> So, the more complete picture of polarization,  $\mathbf{P}$  can be described by,

$$\mathbf{P} = \chi_{ij}^{(1)} \mathbf{E} + \chi_{ijk}^{(2)} \mathbf{E}^2 + \chi_{ijkl}^{(3)} \mathbf{E}^3 + \dots$$

where  $\chi^{(2)}$  and  $\chi^{(3)}$  are the second- and third-order electric susceptibilities, respectively. From this relationship, we can see that the first hyperpolarizability is a third-rank tensor that can be described by a 3x3x3 matrix. Due to Kleinman symmetry, which holds at low frequencies (for a static field  $\omega = 0$ ) and states that susceptibilities are independent of the wavelength interacting fields, the 3D matrix can be reduced to 10 components. Using the x, y, and z components of  $\beta$ ,  $\beta_{total}$  is given by,

$$\beta_{total} = \{(\beta_{xxx} + \beta_{xyy} + \beta_{xzz})^2 + (\beta_{yyy} + \beta_{yzz} + \beta_{yxx})^2 + (\beta_{zzz} + \beta_{zxx} + \beta_{zyy})^2\}^{1/2} \quad (2)$$

The SI unit of  $\beta$  is  $\frac{C^3 m^3}{J^2}$ . For convenience, the reported  $\beta$  values in this work will be expressed in atomic units (a.u.) (1 a.u. =  $3.2063 \times 10^{-53} \frac{C^3 m^3}{J^2}$ ).

To assess the thermal stability of studied molecules, their half-lives ( $t_{1/2}$ ) are considered. Here, we only focus on the ground state ( $S_0$ ) isomerization process where  $t_{1/2}$  signifies the time taken for the concentration of the *Z* isomer to fall to half its initial value. The half-life of each molecule was calculated assuming a first-order reaction and following the first-order rate law, as shown below

$$t_{1/2} = \frac{\ln(2)}{k}. \quad (3)$$

In this relationship,  $k$  represents the rate constant of the reaction and can be obtained following the transition state theory,<sup>35</sup>

$$k(T) = \frac{k_B T}{h c^\circ} e^{-\Delta^\ddagger G^\circ / RT}, \quad (4)$$

where  $k_B$  is the Boltzmann constant,  $k_B = 1.380662 \times 10^{-23}$  J/K,  $T$  is the temperature,  $T = 298.15$  K,  $h$  is the Planck's constant,  $h = 6.626176 \times 10^{-34}$  J s,  $c^\circ$  is the concentration, here  $c^\circ = 1$ ,  $\Delta^\ddagger G^\circ$  is the free activation energy, and  $R$  is the ideal gas constant,  $R = 8.31441$  J/(mol K). Equation (4) shows that there is a significant kinetic component to the calculated thermal half-lives where free energy variations of only 1 kcal/mol can cause a difference in  $t_{1/2}$  of tens of days.

Following the example of Calbo et al.<sup>11</sup>, we use Wiberg indices to establish a relationship between the strength of the azo bond (N=N) of the different molecular geometries and their respective half-lives. The WI measures the density between atoms **A** and **B** and is determined as the sum of the off-diagonal square of the density matrix **P**, where **P** is different than the previously described polarization term,<sup>20</sup>

$$WI_{AB} = \sum_{pA} \sum_{qB} P_{pq}^2. \quad (5)$$

The Wiberg bond index is only one of the parameters provided by the Natural Bond Orbital (NBO) analysis. The NBO analysis is often used to explain the computational solutions of the Schrödinger's wave equation in terms of chemical bonds. NBOs are localized electron pair orbitals for bonding pairs and lone pairs generated from an idealized Lewis structure of the molecule in question. In other words, NBO analysis is based on the optimal transformation of a wave function into a localized form. This localized form corresponds to the bonding pairs, i.e., chemical bonds, and lone pairs of electrons. Here, we use the analyzed electron density expressed in the complete orthonormal set of 1-center localized orbitals — Natural Atomic Orbitals (NAOs). The NAO bond order aspect of the NBO analysis can be used to investigate the electric field effect on the N=N bond character.

## COMPUTATIONAL DETAILS AND METHODOLOGY

Due to high sensitivity of the calculated thermal half-lives to the free energy variations, we compared the response properties of the studied molecules among eight different functionals and three different basis sets. The calculated field-free responses are listed in Table 1, along with the tested functionals. Our results show that B2PLYP functional significantly overestimated the calculated free energies, while BLYP underestimated them. This was expected since the amount of Hartree-Fock (HF) exchange increases from 0% in BLYP to 53% in B2PLYP, resulting in an energy activation barrier increase. The hybrid exchange-correlation PBE0 functional provided  $t_{1/2}$  values the closest to those reported in the literature.<sup>11</sup> All field calculations were computed using CAM-B3LYP, PBE0, and PBE0-D3 functionals. CAM-B3LYP functional was tested based on the Sadley-Sosnowska's work, suggesting that a long-range corrected functional fixes the incorrect electric field dependence modeled by the exchange functional of the traditional DFT methods as B3LYP.<sup>19</sup> Compared to the two PBE0 functionals, CAM-B3LYP vastly overestimated the activation energy barriers ( $\Delta^\ddagger G$ ), as shown in Figure 2, resulting in  $t_{1/2}$  values much higher than anything experimentally observed up to date. Similarly, the addition of Grimme's dispersion correction (D3)<sup>36</sup> to the PBE0 functional also increased the energy activation barriers. This was expected based on the previously reported results, as the dispersion was shown to stabilize the Z isomers of the azoheteroarenes compared to their transition states, leading to an increase in  $t_{1/2}$  with the addition of dispersion.<sup>11</sup> Since the systems under study here are lacking methyl groups, and therefore have less dispersion, the PBE0 functional was used for the primary data collection. Additionally, we decided to use a triple zeta basis set that includes diffuse and polarization functions (6-311+G(d)) to achieve the correct response in the field environment.

**Table 1.** Comparison of the performance of various functionals benchmarked on the field-free **im** type I structure. Results are compared to the experimental half-life of the methylated **im** type I reported by Calbo et al.<sup>11</sup>

Functional	$\Delta^\ddagger G$ (kcal/mol)	$t_{1/2}$ (day)
Experiment	-	<b>6.5</b>
BLYP	22.96	0.1
BLYP-D3	24.79	2.0
B2PLYP	28.71	1471.1
B3LYP	24.44	1.1
B3LYP-D3	25.87	12.1
$\omega$ B97XD	27.97	423.1
PBE0	25.12	3.4
PBE0-D3	25.58	7.5
CAM-B3LYP	26.44	31.5

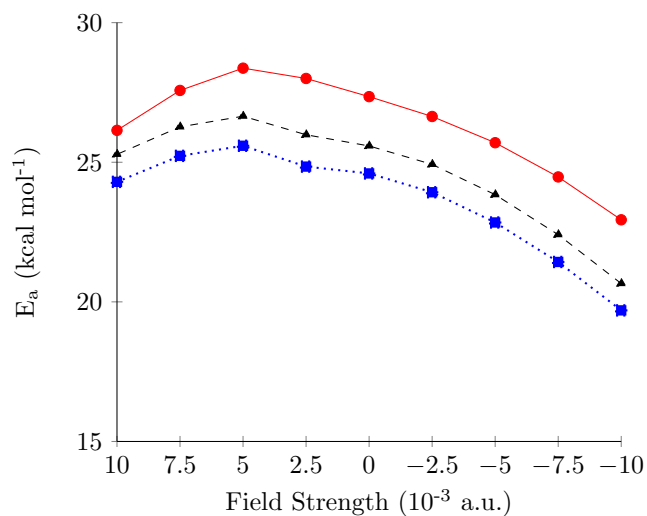


**Figure 2.** Comparison of the performance of various functionals benchmarked on the **im** type I structure in the field environment. Solid red line – CAM-B3LYP, dashed black line – PBE0-D3, dotted blue line – PBE0.

Based on the benchmarking results, we apply the DFT method<sup>33</sup> on the PBE0/6-311+G(d) level of theory, as implemented in the Gaussian 16 suite of programs<sup>34</sup>, for the ground state geometry optimizations, free energy calculations, first hyperpolarizability computations, and Wiberg indices. Relaxed scanning along the -N=N-C bond was employed in the transition state search, after which the intrinsic reaction coordinate (IRC) calculations were used to confirm the accuracy of identified transition states. All calculations were done in gas phase at 25°C, without considering solvent and temperature effects.

All geometry optimizations were first studied in the field-free conditions. The OEEFs were then applied along two different axes, namely  $F_{\text{azo}}$  and  $F_{\text{het}}$ .  $F_{\text{azo}}$  is aligned along an internal coordinate defined by the azo bond and  $F_{\text{het}}$  is oriented along the internal coordinate defined by the N-H bond in the five-membered ring. (Figure 3) The fields were applied in intervals of 0.0025 a.u. from  $\pm 0.0025$  to  $\pm 0.0100$  a.u. ( $1 \text{ a.u.} = 5.14 \times 10^3 \text{ MV cm}^{-1}$ ), following the example of Kempfer-Robertson and Thompson<sup>23</sup>. It should be noted that two different atomic arrangements of the five-membered ring were considered – type I and type II structure of each molecule (Figure 4). This was done to compare the effect of the arrangement of N atoms, within the same system, on that molecule's photoswitching performance.

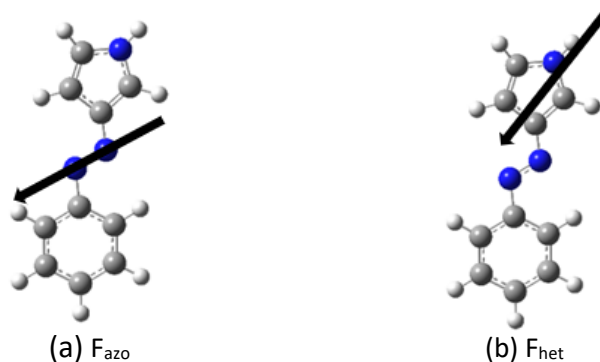


**Figure 3.** OEEF directions demonstrated on the  $S_0$  E isomer of azopyrrole. The arrows are pointing in what will be referred to as the negative field direction. Positive field direction is facing the opposite way.



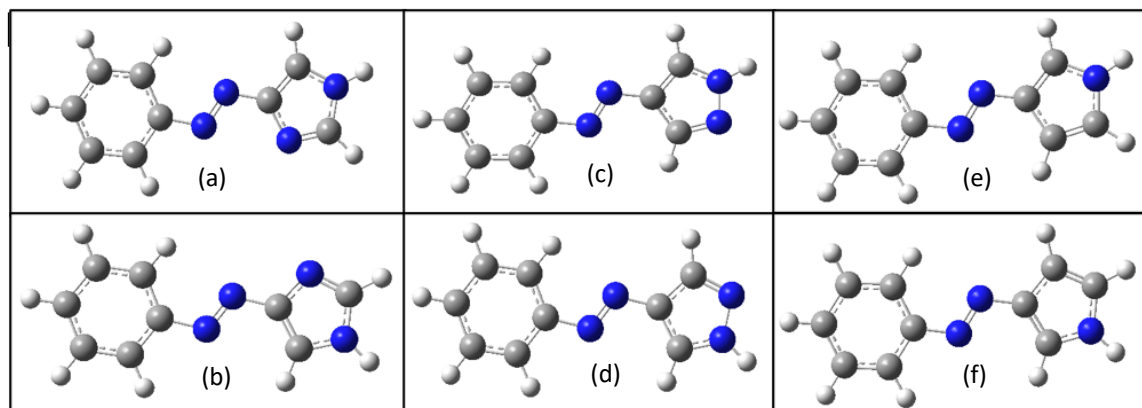


**Figure 4.** Optimized  $S_0$  E isomers of all studied molecules.  
 (a) – **im** type I, (b) – **im** type II, (c) – **pz** type I, (d) – **pz** type II, (e) – **py** type I, (f) – **py** type II

## RESULTS AND DISCUSSION

### Gibbs Reaction Energies of Azoheteroaryl Photoswitches

Four mechanisms have been proposed as possible pathways for the AB photoisomerization – rotation, inversion, concerted inversion, and inversion-assisted rotation.<sup>24</sup> Previous work done on azoheteroaryl photoswitches has shown inversion to be the lowest energy pathway for the thermal isomerization.<sup>11</sup> Computed transition states (TS) and activation barriers for different Z - E isomerization processes confirmed inversion being the preferred pathway for all molecules studied, with the inversion TS  $S_0$  energy values being lower than those of the rotation TS in each case. Optimized  $S_0$  Z and E minima and the TS structures for the two pathways, represented using **im**, are shown in figure 5. In the transition state of the inversion mechanism, one N=N-C angle reaches the value of  $180^\circ$  while the C-N=N-C dihedral angle is  $0^\circ$ . Considering that azoheteroaryl molecules have two different cyclic arrangements of atoms in their structure, there are two possible N=N-C angles that could reach the value of  $180^\circ$ . Initial testing of both possibilities yielded very similar results, so all TS calculations were performed with the N=N-C fragment attached to the

phenyl ring being 180°. It is also common to use multiple isomerization pathways to explain experimental observations when studying AB systems.<sup>29</sup> Stability of the inversion pathway is a consequence of the inversion of an sp<sup>2</sup>-hybridized N orbital, conserving the double bond character of the azo (N=N) group.<sup>23</sup>

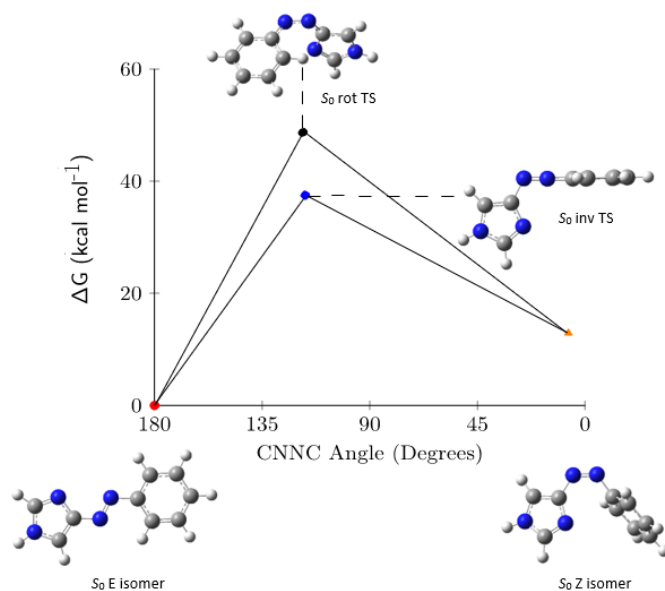


**Figure 5.** Optimized structures of azoimidazole type I  $S_0$  stationary points showing both  $S_0$  rotation and inversion pathways.

Rotation of the rings relative to the azo bridge allows for formation of many different E and Z conformations of heteroaryl systems. Here, only the lowest energy conformers are considered. Since all compounds studied in this work are unsubstituted, they were all found to exhibit a perpendicular T-shaped Z isomer conformation (figure 6), as suggested by previous

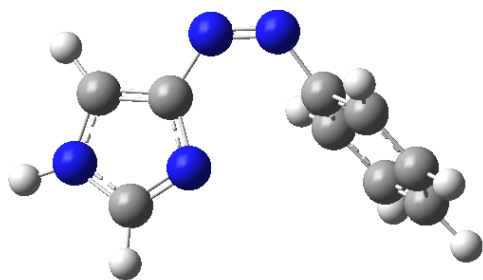


**Figure 6.** Optimized  $S_0$  Z isomer of **im** type I in the T-shaped conformation.

studies.<sup>24</sup> Note that we will refer to the substitution at one or both of the positions of the five-membered heteroarene adjacent to the azo group as *ortho* in this work. A significant difference was noticed in the geometry of the Z isomer of both types of **im** structures compared to the **pz** and **py** Z isomer geometries. In **im**

type I molecule, the *ortho* positioned nitrogen atom with a lone pair (lp) in its  $sp^2$  orbital is facing the benzene ring (Figure 6), and the -N-C-N=N- dihedral angle ( $\varphi$ ) is  $17.1^\circ$ . In **im** type II structure, *ortho* hydrogen interacts with the benzene ring and the -C-C-N=N-  $\varphi$  is  $13.8^\circ$ . Interestingly, type I **im** structure was calculated to be 1.3 kcal/mol lower in energy than its type II counterpart, despite the greater tilt angle. This suggests that in this case, the lp  $\cdots$   $\pi$  interaction is stronger than the C-H  $\cdots$   $\pi$  interaction. Previous studies have demonstrated similar results in aromatic residues of protein structures, and the strong lp  $\cdots$   $\pi$  interaction was explained on the basis of dispersion forces.<sup>30, 31</sup> Molecules **pz** and **py** both have -C-C-N=N-  $\varphi$  angles between  $0.1^\circ$  and  $0.2^\circ$  in all Z geometries. Here, it was noticed that the positioning of the  $sp^3$  nitrogen in the heteroaryl ring influenced Z isomer's geometry. In the case of **pz** and **py** structures, tilt angle reached the value of  $0.2^\circ$  only when the  $sp^3$  N atom was positioned next to the C-H group interacting with the benzene ring (**pz** type II and **py** type I). This had immediate consequences on the stabilization of the Z isomer, with the **pz** type II structure being 0.9 kcal/mol higher in energy than its type I counterpart. In the case of **py**, the difference was more significant, and the type I structure was calculated to be 2.6 kcal/mol higher than the type II structure of the Z isomer. These findings provided first insight into the effects of heteroatom positioning in the five-membered ring on the molecular thermal half-lives. Lone pair in the  $sp^3$  orbital of the  $sp^3$  hybridized N atom provides additional conjugation in the ring, giving the C atom attached to the  $sp^3$  N a higher possibility to bear negative charge, and the formed carbanion leads to the overall destabilization of the molecular system. In terms of conjugation, **pz** and **py** molecules can be described as having "partial" conjugation with respect to the azo bond, i.e., the entire molecular system is not conjugated with the azo group and the phenyl ring. On the other hand, **im** has "complete" conjugation with respect to the azo bond and the phenyl ring. This is only true in their E isomers. As mentioned previously,

Z isomer is oriented so that the phenyl and heteroaryl rings are, essentially, perpendicular to one another, preventing the conjugation with the phenyl ring.<sup>32</sup>

Application of electric fields in certain directions was able to change the overall geometry of inversion transition state (inv TS). In some cases, the N=N-C fragment of the inv TS structure, attached to the phenyl ring, is still at 180°, but as the greater magnitude field is applied, the phenyl ring rotates to become planar as opposed to perpendicular with respect to the heterocyclic ring. This phenomenon appeared in the inv TS structures of all molecules, only in the negative direction of either of the two fields. When the azo and het fields are applied in the negative direction, regardless of the molecular system, they both cause the electron density to relocate from the heterocyclic ring in the direction of the phenyl moiety (Figure 3). However, there appears to be a threshold which when crossed, the phenyl ring reorients to become planar in the inv TS, stabilizing the system and decreasing the overall Gibbs activation energy ( $\Delta^\ddagger G$ ).

Tables S1-S12 show calculated Gibbs reaction energies ( $\Delta G$ ) for all molecules, with respect to their field-free E isomer's energies. Graphical representation of Z isomer's  $\Delta G$  values can be found in Figures 7-9.

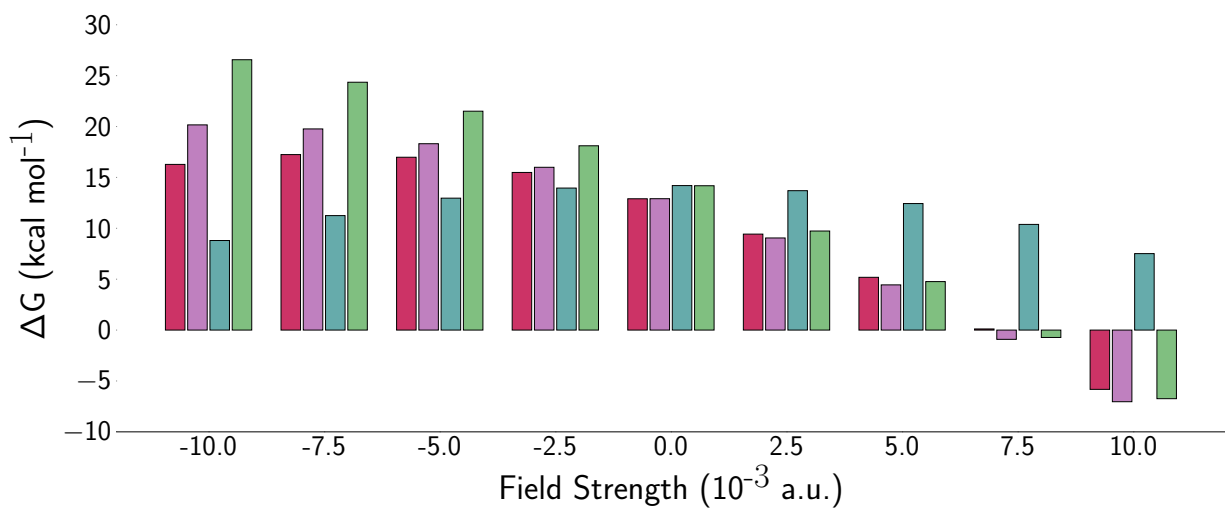


**Figure 7.** Reaction Gibbs energy for the  $S_0$  Z isomer of azoimidazole, with respect to the E isomer, as a function of field strength. Pink – im type I  $F_{\text{azo}}$ , purple - im type I  $F_{\text{het}}$ , dark green - im type II  $F_{\text{azo}}$ , light green - im type II  $F_{\text{het}}$ .

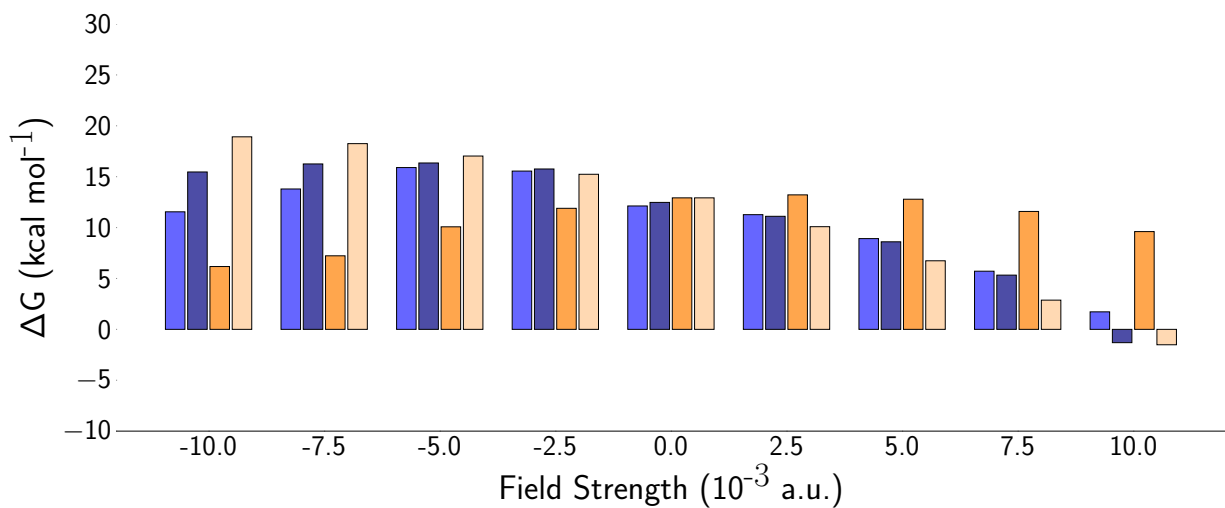


**Figure 8.** Reaction Gibbs energy for the  $S_0$  Z isomer of azopyrazole, with respect to the E isomer, as a function of field strength. Light blue – **pz** type I  $F_{\text{azo}}$ , dark blue - **pz** type I  $F_{\text{het}}$ , dark orange - **pz** type II  $F_{\text{azo}}$ , light orange - **pz** type II  $F_{\text{het}}$ .

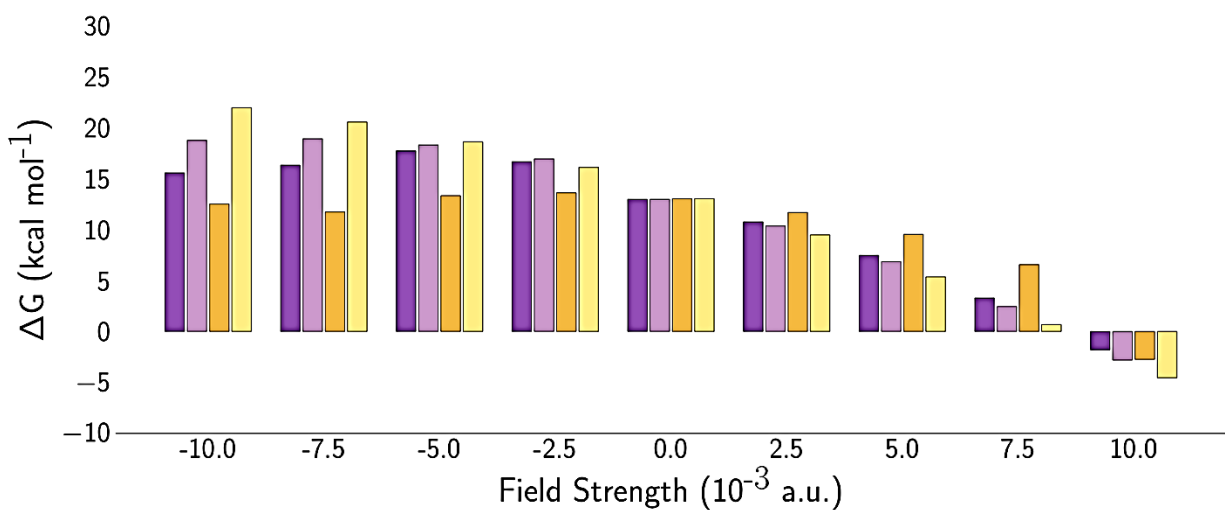


**Figure 9.** Reaction Gibbs energy for the  $S_0$  Z isomer of azopyrrole, with respect to the E isomer, as a function of field strength. Dark purple – **py** type I  $F_{\text{azo}}$ , light purple - **py** type I  $F_{\text{het}}$ , dark yellow - **py** type II  $F_{\text{azo}}$ , light yellow - **py** type II  $F_{\text{het}}$ .

First, we elaborate the  $F_{\text{azo}}$  effects on  $\Delta G$  of each system. Positive  $F_{\text{azo}}$  stabilized all Z isomers of the studied molecules while negative  $F_{\text{azo}}$  had various effects on the molecular systems. In the case of **im**, negative  $F_{\text{azo}}$  stabilized the Z isomer of the type II molecule but destabilized type I molecule's Z isomer. The **pz** type II Z isomer was stabilized by negative  $F_{\text{azo}}$ , while its type I structure was destabilized. Z isomer of the **py** type II molecule was destabilized by negative  $F_{\text{azo}}$ , and its type I counterpart was stabilized only when the -0.0075 a.u. and -0.0100 a.u. field magnitudes were applied. The E isomer was primarily stabilized by the positive  $F_{\text{azo}}$  in all molecules. The only exception is the type II **pz** E isomer, which was only stabilized once the higher field magnitudes were applied (0.0075 a.u.). The inversion transition state (inv TS) was stabilized by the positive  $F_{\text{azo}}$  in all cases. All type II E isomers were stabilized under the application of negative  $F_{\text{azo}}$  while the opposite was true for all type I structures. A similar trend was noticed for the inv TS under the application of the negative  $F_{\text{azo}}$ .

Now, we turn to the effects of  $F_{\text{het}}$  on  $\Delta G$  values. Figures 7-9 should, once again, be referred to for the visual representation of the observed field effects on the  $\Delta G$  values of the Z isomer. In general, application of  $F_{\text{het}}$  in the positive direction stabilized every molecular system studied, while the negative  $F_{\text{het}}$  direction destabilized each structure. This was entirely true for the Z isomers and inv TS geometries, however, E isomers showed some deviation from this trend when the **pz** and **py** molecules were studied. In the case of both **pz** structures, the molecules were stabilized after the -0.0050 a.u. field was applied.

Both fields were shown to stabilize the Z isomers of the studied molecules using certain field magnitudes and directions. Some Z isomers were stabilized by as much as 7 kcal/mol (**py**, type II, +0.0100 a.u.  $F_{\text{azo}}$ ), while the highest calculated energetic destabilization was by 10

kcal/mol (**pz**, type II, -0.0100 a.u.  $F_{\text{het}}$ ), in reference to the Z isomer's free energy value in the field-free environment.

### Dipoles and First Hyperpolarizabilities of Azoheteroaryl Photoswitches

In the field-free environment,  $S_0$  E structure is planar in all three molecules, **im**, **pz**, **py**, and their respective total dipole moments ( $\mu_{\text{tot}}$ ) were calculated to be 4.2 D, 2.3 D, and 3.1 D. The full point group of these molecular systems is C1, indicating no symmetry in any case.  $S_0$  Z structures were calculated to have total dipole moment values of 6.7 D, 3.9 D, and 5.5 D for **im**, **pz**, and **py**, respectively. Table 2 shows calculated first hyperpolarizabilities ( $\beta_{\text{tot}}$ ) for all structures in the field-free environment, as well as the relevant bond lengths of the inv TS. Figure 10 shows the optimized  $S_0$  inv TS structure showing NN and NC bonds.

**Table 2.** Total first hyperpolarizabilities calculated for the E and Z isomers and inv TS of the studied molecules in the field-free environment, along with NN and NC bond lengths of inv TS.

Molecule	Type	$\beta_{\text{tot}}$ E isomer (a.u.)	$\beta_{\text{tot}}$ Z isomer (a.u.)	$\beta_{\text{tot}}$ inv TS (a.u.)	NN bond length (Å)	NC bond length (Å)
Azoimidazole	I	168	148	710	1.2155	1.3226
	II	140	109	1090	1.2172	1.3230
Azopyrazole	I	79	107	145	1.2177	1.3248
	II	60	56	50	1.2176	1.3242
Azopyrrole	I	134	124	564	1.2188	1.3219
	II	112	94	502	1.2184	1.3214

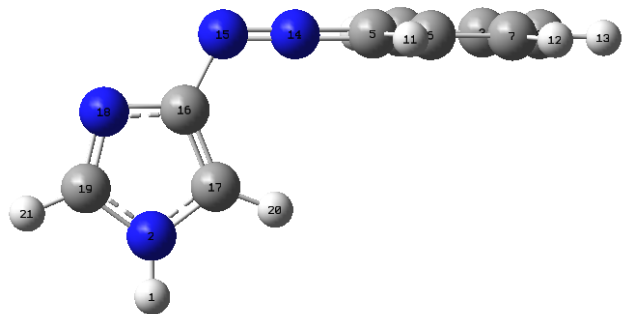


**Figure 10.** Optimized  $S_0$  inv TS of **im** type II showing N14=C5 of the  $F_{\text{het}}$  atom arrangement.

Observing each molecular system separately, with its two types, our results show that structures with highest  $\beta_{\text{tot}}$  inv TS also have the longest NN and NC bonds. For **im** structures, type II inv TS was calculated to have  $\beta_{\text{tot}}$  of 1090 a.u., about 1.5 times greater than inv TS  $\beta_{\text{tot}}$  of type I. **Im** type I was also found to have

longer NN and NC bonds than its type II counterpart. Similarly, in the case of **pz** molecules, type I has inv TS  $\beta_{\text{tot}}$  value almost 3 times greater than the type II structure, and the type I's NN and NC bonds were calculated to be longer than those of type II. Finally, the same trend was noticed for the **py** systems, with the type I structure showing higher inv TS  $\beta_{\text{tot}}$  and longer NN and NC bonds. Longer NN and NC bond lengths imply lower p character of these bonds which is further connected to lower strength of those connections. It would be expected that molecules that exhibit weaker double bonding in the inv TS give a higher potential for a dipole to be induced in those systems.

Figures 11 (a)-(c) illustrate observed trends regarding the  $\beta_{\text{tot}}$  values for each system in the field environment. Beginning with  $F_{\text{azo}}$ , when applied in the positive direction, this field caused an increase in both,  $\mu_{\text{tot}}$  and  $\beta_{\text{tot}}$  of all Z isomers. In the case of **im**, negative  $F_{\text{azo}}$  increased type II's  $\mu_{\text{tot}}$  and  $\beta_{\text{tot}}$ , but decreased type I's  $\mu_{\text{tot}}$  and  $\beta_{\text{tot}}$  values. An increase in  $\mu_{\text{tot}}$  and  $\beta_{\text{tot}}$  was noticed for both structural types of **pz**. Z isomer of the **py** type II molecule showed a decrease in its  $\mu_{\text{tot}}$  and  $\beta_{\text{tot}}$  under negative  $F_{\text{azo}}$ . Its type I counterpart showed an increase in  $\mu_{\text{tot}}$  and  $\beta_{\text{tot}}$  values only when the -0.0075 a.u. and -0.0100 a.u. field magnitudes were applied. This is an example of a strong-



field dipole-inversion effect where due to the strength of the electric field, the dipole vector realigns to be antiparallel to the applied field.<sup>23</sup>

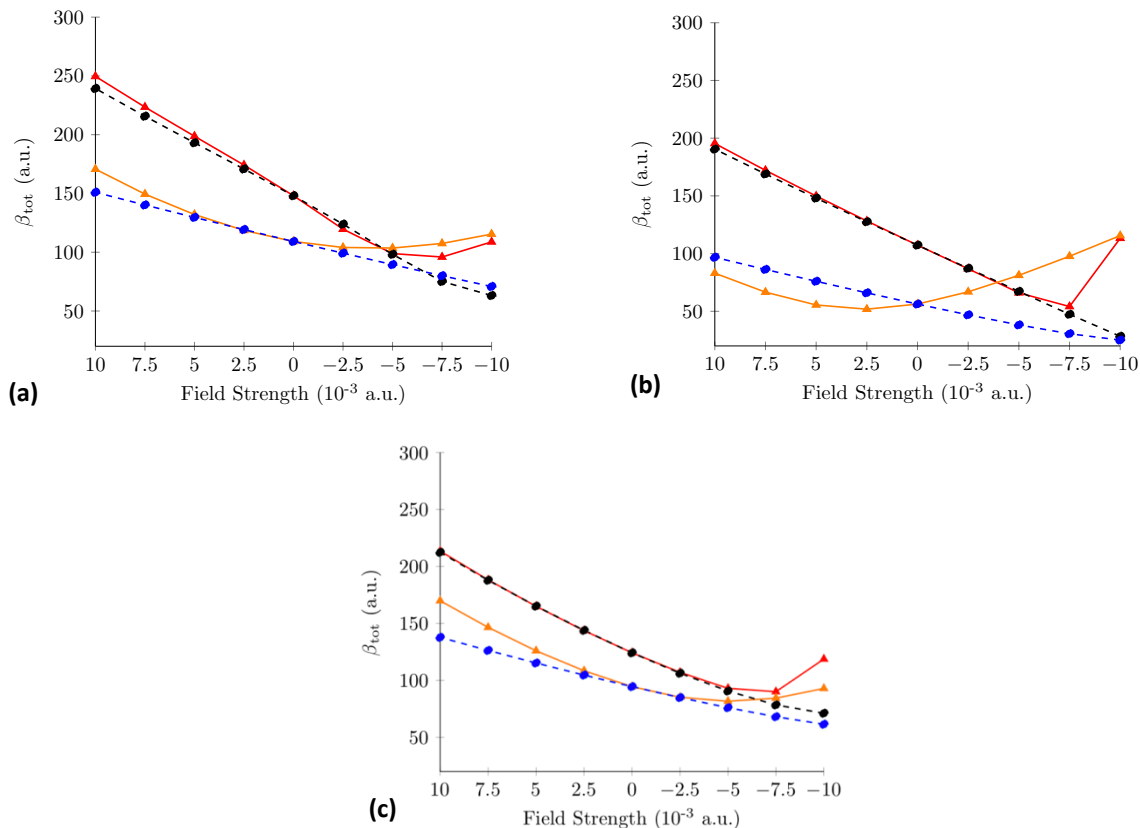


**Figure 11.** Total first hyperpolarizability as a function of field strength. Solid red line – type I  $F_{\text{azo}}$ , solid orange line – type II  $F_{\text{azo}}$ , dashed black line – type I  $F_{\text{het}}$ , dashed blue line – type II  $F_{\text{het}}$ . **(a)** – **im**, **(b)** – **pz**, **(c)** – **py**.

The  $\mu_{\text{tot}}$  trends follow the general notion of energetic stabilization offering higher total dipole values and vice versa.  $\mu_{\text{tot}}$  and  $\beta_{\text{tot}}$  values for the E isomer increased in all systems when positive  $F_{\text{azo}}$  was applied.  $\mu_{\text{tot}}$  and  $\beta_{\text{tot}}$  of inv TS also increased with this field direction, except for the  $\beta_{\text{tot}}$  values of the **im** structures which decreased. Under the application of negative  $F_{\text{het}}$ ,  $\beta_{\text{tot}}$  values decreased for most E isomers, with the exception of the **pz** type II structure. The inv TS showed an increase in  $\beta_{\text{tot}}$  for both **im** molecules and the **pz** type II structure, and a decrease in  $\beta_{\text{tot}}$  for both **py** molecules and the **pz** type I structure.

As for the  $F_{\text{het}}$  effects, in general, positive  $F_{\text{het}}$  direction increased the  $\mu_{\text{tot}}$  values for all molecules while the negative direction decreased them. Values of  $\beta_{\text{tot}}$  were increased by the positive  $F_{\text{het}}$  direction for all E and Z isomers but decreased for some inv TS structures (**im** type I, type II and **py** type II). Opposite trend was observed once the negative direction of  $F_{\text{het}}$  was applied. Overall, the highest increase in  $\mu_{\text{tot}}$  was noted to be of 4.5 D (**im**, type I, +0.0100 a.u.  $F_{\text{azo}}$ ), while the highest increase in  $\beta_{\text{tot}}$  was calculated to be of 100 a.u (**im**, type I, +0.0100 a.u.  $F_{\text{azo}}$ ) compared to the field-free values of the particular Z isomer. A clearer structure of the observed trends can be noticed with the application of an electric field along one of the N-H bonds in each structure, as opposed to general trends noticed when  $F_{\text{azo}}$  was used. In comparison to  $F_{\text{azo}}$ ,  $F_{\text{het}}$  initiates a more uniform response from the azoheteroarenes studied in this work and would likely be a better experimental tool for studying their nonlinear optical properties.

### Gibbs Activation Energies and Thermal Half-Lives of Azoheteroaryl Photoswitches

**Table 3.** Thermal half-lives calculated for the studied molecules in the field-free environment as compared to the experimental half-lives calculated for the methylated derivatives.

Molecule	Type	$t_{1/2}$ (day)	Experimental <sup>1</sup> $t_{1/2}$ (day)
Azoimidazole	I	1.4	6.5
	II	4.7	
Azopyrazole	I	134.6	1000
	II	52.4	
Azopyrrole	I	5.7	3.7
	II	7.8	

Given that the reaction kinetics were calculated according to the transition state theory, previously described Z isomer free energy deviations had a significant impact on the calculated field-free half-lives. Table 3 shows the obtained  $t_{1/2}$  values for both Z geometries of each molecule. It should be noted that  $t_{1/2}$  is a property of  $\Delta^\ddagger G$ , hence the two are discussed together.

<sup>1</sup> Structures of methylated derivatives can be found in Ref. [11].

Tables S13 and S14 show calculated  $\Delta^\ddagger G$  values for all studied systems. In the case of **pz** and **py**, the more stable Z isomers were calculated to have longer thermal half-lives in the field-free environment, 134.6 days (**pz**, type I) and 7.8 days (**py**, type II). The **im** molecule offered the lowest thermal half-life of 4.7 days for its type II Z isomer geometry. Table 3 also includes the previously reported experimental values of similar molecules that include methyl substituents, obtained by Calbo et al.<sup>11</sup> Even without the electric field applied, the unsubstituted **py** molecule offered a higher theoretical thermal half-life than the trisubstituted pyrrole heteroarene molecule ( $t_{1/2} = 3.7$  days) in the previously mentioned study. To the best of our knowledge, no previous reports on the experimental half-lives of the studied molecules exist, so we are unable to deduce the exact comparison between the theoretical and experimental trends. Nonetheless, the field-free  $t_{1/2}$  results support the previously established advantage of azopyrazole's geometry as related to its kinetics.<sup>11</sup> Pyrazoles are the worst electron-donors to the azo group in comparison to pyrroles and imidazoles. Partial conjugative electron donation of azopyrazoles results in a higher double-bond character of the azo bridge, giving a more stable Z isomer that takes a longer time to isomerize to the E isomer. A note should be made on the connection between  $t_{1/2}$  and nonlinear optical properties of these molecules. For example, **pz** type I molecule offers a great theoretical  $t_{1/2}$  but its  $\beta_{\text{tot}}$  values are not as high as those calculated for the **im** molecules. While, on the other hand, **im** molecules did not offer as large  $t_{1/2}$  values. These findings suggest that the trade-off between kinetic performance and the ability to induce a dipole in a particular molecular system should be taken into consideration prior to development of a molecular switch.

We will now examine the effects of  $F_{\text{azo}}$  on  $\Delta^\ddagger G$  and  $t_{1/2}$  values. Table 4 contains all calculated  $t_{1/2}$  values under the application of  $F_{\text{azo}}$ .

**Table 4.** Thermal half-lives reported in days for all molecules under the application of  $F_{\text{azo}}$ .

Molecule	Type	-0.0100 a.u.	-0.0075 a.u.	-0.0050 a.u.	-0.0025 a.u.	0.0000 a.u.	0.0025 a.u.	0.0050 a.u.	0.0075 a.u.	0.0100 a.u.
im	I	0.8	4.0	7.4	2.1	1.4	0.4	0.1	0	0
	II	0.4	3.6	45.1	5.1	4.6	1.9	0.4	0	0
pz	I	122.0	214.7	25.1	3.1	134.6	4.8	0.3	0	0
	II	0.6	224.7	238.2	78.1	52.4	14.5	2.1	0.2	0
py	I	1.5	9.2	0.7	0.5	5.7	0.7	0.1	0	0
	II	0.1	58.4	16.9	14.3	7.8	2.1	0.3	0	0

We will focus on the most notable findings as compared to the field-free values. Overall, the negative direction of  $F_{\text{azo}}$  increased  $t_{1/2}$  values of all studied molecules while the positive direction did the opposite. The only exception was found to be the type II structure of **py** for which the trend was reversed. A clear correlation to the observed  $\Delta G$  trends is seen among the data presented in Table 4, with there existing a threshold field value for each molecule, after which the molecule stabilizes, and its  $t_{1/2}$  starts decreasing. Two most commonly observed electric field threshold magnitudes are 0.0050 a.u. and 0.0075 a.u.

Examining the **im** molecule, type II structure was noted to have a higher field-free  $t_{1/2}$  than the type I structure. Theoretical calculations show that once the 0.0050 a.u. field is applied along the azo bond in the negative direction, **im** type II structure's  $t_{1/2}$  reaches 45.1 days, a value almost 10 times greater than the calculated field-free one. This increase in length of  $t_{1/2}$  of **im** was followed by a 1.35 kcal/mol increase in  $\Delta^{\ddagger}G$ . In the case of **pz** molecule, its type I structure retained the highest  $t_{1/2}$  in the field-free environment, but the type II structure's  $t_{1/2}$  was raised to 238.2 days with the application of the 0.0050 a.u. field along the azo group in the negative direction. It should be noted that the field-free  $t_{1/2}$  of **pz** type I does not follow the general trend observed in other molecules, in terms of the  $t_{1/2}$  values increasing or decreasing in a specific direction. Compared to

the type II structure's field-free  $t_{1/2}$  of 52.4 days, application of the electric field increased type II's  $t_{1/2}$  by 4.5 times, while  $\Delta^\ddagger G$  was raised by 0.89 kcal/mol. Finally, looking at the **py** molecule, our calculations showed that with the application of 0.0075 a.u. field in the negative direction,  $t_{1/2}$  of this molecule could be increased to 58.4 days, with its  $\Delta^\ddagger G$  increasing by 1.19 kcal/mol. All calculated  $t_{1/2}$  value should be taken with a dose of uncertainty due to the intricate nature of the transition state theory calculations, where even minuscule variations in the activation barrier of less than 1 kcal/mol can change  $t_{1/2}$  values by an order of magnitude. Nonetheless, even the **py** type II structure was improved in terms of its  $t_{1/2}$  which rose to 9.2 days once the 0.0075 a.u. field was applied in the negative direction, while its  $\Delta^\ddagger G$  was increased by 0.29 kcal/mol. Now we can see that, even though the exact half-lives should be confirmed experimentally, the OEEFs can certainly be used to tune the kinetics of the thermal isomerization of unsubstituted azoheteroarenes and bring them to a level comparable to their methylated derivatives.

Turning to the effects of  $F_{\text{het}}$ , detailed  $t_{1/2}$  values for this field can be found in Table 5.

**Table 5.** Thermal half-lives reported in days for all molecules under the application of  $F_{\text{het}}$ .

Molecule	Type	-0.0100 a.u.	-0.0075 a.u.	-0.0050 a.u.	-0.0025 a.u.	0.0000 a.u.	0.0025 a.u.	0.0050 a.u.	0.0075 a.u.	0.0100 a.u.
im	I	0	0.9	4.7	25.4	1.4	0.3	0	0	0
	II	0.2	0.2	0.6	1.7	4.6	12.6	34.1	94.3	254.9
pz	I	0.1	2.8	10.3	2.6	134.6	6.4	0.5	0	0
	II	0.4	1.8	5.4	17.0	52.4	153.8	437.6	1222.5	3185.0
py	I	0.1	1.6	13.2	0.8	5.7	0.5	0	0	0
	II	0.1	0.3	0.8	2.4	7.8	22.9	74.5	256.6	889.7

In terms of the overall kinetics of the isomerization process, negative  $F_{\text{het}}$  direction consistently lowered  $t_{1/2}$  values of all molecules, while the positive  $F_{\text{het}}$  direction offered varying results for different systems. In **im**, type I structure's  $t_{1/2}$  were decreased in the positive direction, while its counterpart, type II, showed an overall increase once this field direction was used. The highest calculated  $t_{1/2}$  for **im** was 254.9 days, achieved when the +0.0100 a.u.  $F_{\text{het}}$  was applied to the type II structure. This  $t_{1/2}$  value is approximately 54 times higher than the  $t_{1/2}$  calculated in the field-free environment. The  $\Delta^\ddagger G$  was raised by 2.37 kcal/mol. Compared to the highest  $t_{1/2}$  value calculated for **im** with the  $F_{\text{azo}}$  application ( $t_{1/2, \text{azo}} = 45.1$  days), orientation of the electric field along the N-H bond increased  $t_{1/2}$  by over 5 times. A significant increase in the  $t_{1/2}$  for the **pz** type II molecule was achieved by application of +0.0100 a.u.  $F_{\text{het}}$  field, with the calculated  $t_{1/2}$  being 3185 days, a value 61 times greater than the calculated field-free  $t_{1/2}$  of 52.4 days. Increase in the calculated  $t_{1/2}$  was followed by a 2.44 kcal/mol increase in  $\Delta^\ddagger G$ . In the case of **py** molecule,  $t_{1/2}$  of its type II structure showed the highest calculated value of 889.7 days upon the application of positive 0.0100 a.u.  $F_{\text{het}}$ , a value 114 times greater than the calculated  $t_{1/2}$  in the field-free environment ( $t_{1/2, \text{field-free}} = 7.8$  days). As mentioned previously,  $F_{\text{azo}}$  application increased the **py**  $t_{1/2}$  to 58.4 days, which is about 15 times lower than the value obtained by the  $F_{\text{het}}$  application. This increase in  $t_{1/2}$  was followed by a 2.81 kcal/mol increase in  $\Delta^\ddagger G$ .

### Wiberg Indices as They Relate to the Isomerization kinetics

To further investigate the OEEF effects on isomerization kinetics of azoheteroarenes, we discuss one aspect of NBO analysis – Wiberg bond indices (WIs) – as it relates to the calculated  $t_{1/2}$  values. Based on the work done by Calbo et al., higher WI values should be representative of higher  $t_{1/2}$  values, and vice versa.<sup>11</sup> This was deemed partially true based on the results discussed here. Focusing on the inv TSs, we calculated WIs for the NN and NC bonds (figure 10) in each

molecular system. Table 6 lists the highest calculated  $t_{1/2}$  values for each molecule, along with the field conditions at which those values are achieved, NN and NC bond lengths, and their respective WIs.

**Table 6.** Highest thermal half-lives calculated for the studied molecules in the field environment along with the NN and NC bond lengths of their inv TSs and their respective WIs.

Molecule	Type	Conditions	$t_{1/2}$ (day)	NN bond length (Å)	NC bond length (Å)	NN WI	NC WI
im	I	$F_{\text{het}} -0.0025$ au.	25.4	1.2155	1.3275	1.8566	1.2159
	II	$F_{\text{het}} +0.0100$ au.	254.9	1.2209	1.3203	1.8298	1.2394
pz	I	$F_{\text{azo}} -0.0075$ au.	214.7	1.2212	1.3366	1.8556	1.1863
	II	$F_{\text{het}} +0.0100$ au.	3185.0	1.2282	1.3207	1.8187	1.2375
py	I	$F_{\text{het}} -0.0050$ au.	13.2	1.2170	1.3327	1.8411	1.2101
	II	$F_{\text{het}} +0.0100$ au.	889.7	1.2229	1.3198	1.8072	1.2437

When comparing type I and type II values for each molecular system, it can be observed that molecules with higher  $t_{1/2}$  values, also have higher NC WIs and lower NN WIs. For example, in the case of **im** type I and type II molecules, type II was calculated to have a  $t_{1/2}$  value of about 255 days, whereas type I was found to have a  $t_{1/2}$  of 25 days. Observing their WIs, type II structure has a higher NC WI of 1.2394, compared to an NC WI of 1.2159 for the type I structure. On the other hand, NN WI was calculated to be lower for the type II structure (1.8298) and higher for the type I structure (1.8566). A similar trend is observed for every molecular system studied. Higher  $t_{1/2}$  values are correlated with higher NC WIs. This suggests that the more electron density is relocated towards the heterocyclic moiety, the NC bond in particular, the higher the thermal

stability of the particular system. This is also confirmed by the general trend regarding the field conditions that afforded the highest  $t_{1/2}$  values – positive  $F_{\text{het}}$  of greater magnitudes (0.0075 a.u. and 0.0100 a.u.) provided the longest  $t_{1/2}$ . Another interesting finding was the connection between the positioning of the N-H bond along which the  $F_{\text{het}}$  was applied and the calculated  $t_{1/2}$  values. Figure 12 shows the optimized  $S_0$  Z isomers of all molecules. From this illustration, it can be noticed that all structural types that were found to have a dominant  $t_{1/2}$  over the other, have their N-H bonds almost perpendicular to the N=N bond (figure 12 b, d, e). Positive  $F_{\text{het}}$  direction is, essentially, aiding in electron density relocation from the N=N bond towards the heterocyclic moiety, in a perpendicular fashion. This is the case in **im** type II, **pz** type II, and **py** type I molecules, all of which were calculated to have higher  $t_{1/2}$  than the other type of the same molecular classification. These results suggest that the application of an electric field perpendicular to the azo bond, in the sense of an internal molecular coordinate, stimulates a higher degree of partial conjugation in the molecule, which in turn leads to a longer thermal half-life of that system.

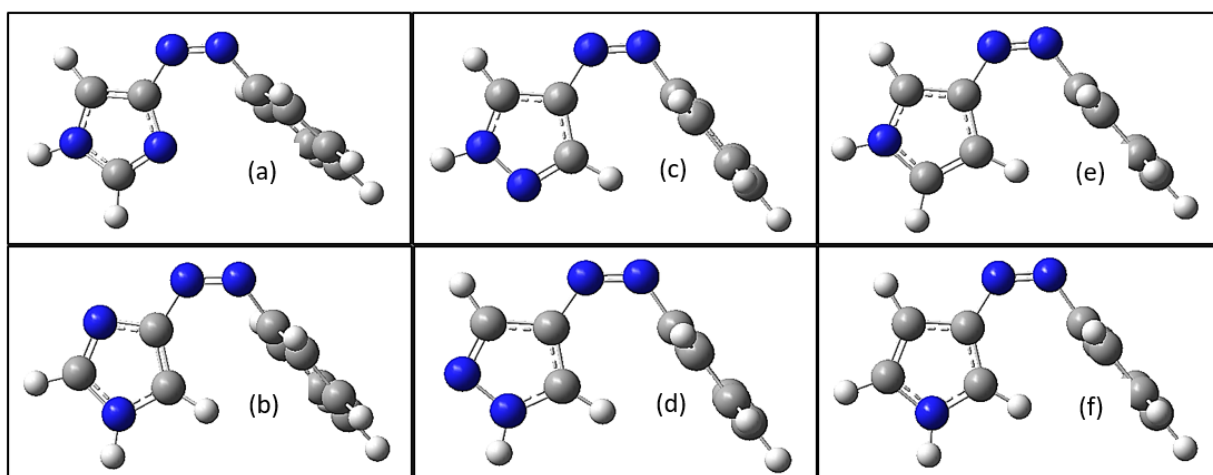


**Figure 12.** Optimized  $S_0$  Z isomers of all studied molecules.  
 (a) – **im** type I, (b) – **im** type II, (c) – **pz** type I, (d) – **pz** type II, (e) – **py** type I, (f) – **py** type II



Overall,  $F_{\text{het}}$  showed to increase the NC WIs of the inv TSs more than  $F_{\text{azo}}$  did, suggesting that the internal coordinate defined by the N-H bond may be a better choice in terms of the OEEF tuning potential. Even though an experimentalist may not be able to directly manipulate the transition state of the particular isomerization reaction, knowing how the electric fields will affect this structure can help determine what initial conditions can be applied on the starting isomer to increase the overall  $t_{1/2}$  of the preferred state. If the molecule is tethered to a surface, the orientation, with respect to the field, is well defined, so electric fields can effectively be used in a photoswitching device.

## CONCLUSIONS

In this work, we examined how OEEFs can be used to tune the photoswitching properties of three unsubstituted heteroaryl azo compounds — azoimidazole (**im**), azopyrazole (**pz**), and azopyrrole (**py**). Based on a density functional theory approach, the electric field control of the thermal relaxation time and nonlinear optical properties of **im**, **pz**, and **py** was examined. Wiberg indices and appropriate bond lengths were used to explain the correlation between the observed half-life ( $t_{1/2}$ ) trends and the electric field effects. The results of our study show that favorable OEEF orientations can increase the  $t_{1/2}$  values of the studied molecules by as much as 60 times, compared to their  $t_{1/2}$  values in the field-free environment. For example, the application of an electric field along an internal coordinate defined by the N-H bond of an arylazopyrazole molecule at a magnitude of 0.0100 a.u. yielded a theoretical  $t_{1/2}$  value of approximately 3000 days. These findings show that OEEFs can be used to tune the kinetics of the thermal isomerization of unsubstituted azoheteroarenes and bring them to a level comparable to their methylated derivatives. To achieve slower Z – E isomerization kinetics, the activation energy barrier ( $\Delta^\ddagger G$ ) was only raised by 2.4 kcal/mol. In addition, certain OEEF magnitudes were found to increase

total first hyperpolarizabilities of some azoheteroarenes by as much as 100 a.u., as was the case with the arylazoimidazole molecule. The OEEFs offered a possibility of controlling the energy activation barrier heights for the thermal isomerization process as some *Z* isomers were stabilized by as much as 7 kcal/mol, while the highest calculated energetic destabilization was by 10 kcal/mol, in reference to the *Z* isomer's free energy value in the field-free environment.

## REFERENCES

- 1) Sauvage, J.-P., Ed. *Molecular Machines and Motors; Structure and Bonding*. Springer: Berlin, Heidelberg **2001**, 99.
- 2) Martins G. F., Cabral, B. J. C. Electron Propagator Theory Approach to the Electron Binding Energies of a Prototypical Photo-Switch Molecular System: Azobenzene. *J. Phys. Chem. A* **2019**, *123*, 10, 2091–2099.
- 3) Crecca, C. R., & Roitberg, A. E. Theoretical study of the isomerization mechanism of azobenzene and disubstituted azobenzene derivatives. *J. Phys. Chem. A* **2006**, *110*(26), 8188–8203.
- 4) Mahimwalla, Z., Yager, K. G., Mamiya, J., Shishido, A., Priimagi, A., Barrett, C. J. Azobenzene photomechanics: prospects and potential applications. *Polym. Bull.* **2012**, *69*, 967–1006.
- 5) Pirone, D.; Bandeira, N.A.G.; Tylkowski, B.; Boswell, E.; Labeque, R.; Garcia Valls, R.; Giamberini, M. Contrasting Photo-Switching Rates in Azobenzene Derivatives: How the Nature of the Substituent Plays a Role. *Polymers* **2020**, *12*, 1019.
- 6) Liu, Z. F., Hashimoto K., & Fujishima, A. Photoelectrochemical information storage using an azobenzene derivative. *Nature* **1990**, *347*, 658–660.
- 7) Hvilsted, S., Sa'nchez, C., & Alcalá, R. The volume holographic optical storage potential in azobenzene containing polymers. *J. Mater. Chem.* **2009**, *19*, 6641–6648.
- 8) Yu, Y., Nakano, M., & Ikeda, T., Directed bending of a polymer film by light. *Nature* **2003**, *425*, 145.
- 9) Muraoka, T., Kinbara, K., & Aida, T. Mechanical twisting of a guest by a photoresponsive host. *Nature* **2006**, *440*, 512–515.
- 10) Yamada, M., Kondo, M. Mamiya, J., Yu, Y., Kinoshita, M., Barrett, C. J., & Ikeda, T. Photomobile Polymer Materials: Towards Light-Driven Plastic Motors. *Chem., Int. Ed.* **2008**, *47*, 4986–4988.
- 11) Calbo, J., Weston, C. E., White, J. P., Rzepa, H. S., Contreras-García, J., & Fuchter, M. J. Tuning Azoheteroarene Photoswitch Performance through Heteroaryl Design. *J. Am. Chem. Soc.* **2017**, *139*, 3, 1261–1274.
- 12) Wang, Y., Liu X., Cui G., Fang, W., Thiel, W. Photoisomerization of Arylazopyrazole Photoswitches: Stereospecific Excited-State Relaxation. *Angew. Chem. Int. Ed.* **2016**, *55*, 14009.
- 13) Weston, C. E., Richardson, R. D., Haycock, P. R., White, A. J. P., & Fuchter, M. J. Arylazopyrazoles: Azoheteroarene Photoswitches Offering Quantitative Isomerization and Long Thermal Half-Lives. *J. Am. Chem. Soc.* **2014**, *136*, 34, 11878–11881.
- 14) Stricker, L., Fritz, E., Peterlechner, M., Doltsinis, N. L., & Ravoo, B. J. Arylazopyrazoles as Light-Responsive Molecular Switches in Cyclodextrin-Based Supramolecular Systems. *J. Am. Chem. Soc.* **2016**, *138* (13), 4547-4554.

- 15) Otsuki, J., Suwa, K., Narutaki, K., Sinha, C., Yoshikawa, I., & Araki, K. Photochromism of 2-(Phenylazo)imidazoles. *J. Phys. Chem. A* **2005**, *109* (35), 8064–8069.
- 16) Fuchter, M. J. On the Promise of Photopharmacology Using Photoswitches: A Medicinal Chemist's Perspective. *J. Med. Chem.* **2020**, *63*, 20, 11436–11447.
- 17) Beharry, A., & Woolley, A. Azobenzene photoswitches for biomolecules. *Chem. Soc. Rev.* **2011**, *40*, 4422–4437.
- 18) Shaik, S., Mandal, D. & Ramanan, R. Oriented electric fields as future smart reagents in chemistry. *Nature Chem* **2016**, *6*, 1091–1098.
- 19) Sadlej-Sosnowska, N. The response of electronic and energetic properties of conjugated vs aromatic molecules to an external uniform electric field. *Structural Chemistry* **2019**, *30*, 1407–1413.
- 20) Wiberg, K. B. Application of the pople-santry-segal CNDO method to the cyclopropylcarbiny and cyclobutyl cation and to bicyclobutane. *Tetrahedron* **1968**, *24*, 1083– 1096.
- 21) Conti, I., Garavelli, M., Orlandi, G. The different photoisomerization efficiency of azobenzene in the lowest  $\pi\pi^*$  and  $\pi\pi^*$  singlets: The role of a phantom state. *J. Am. Chem. Soc.* **2008**, *130*, 5216–5230.
- 22) El-Tahawy, M. M. T., Nenov, A., Weingart, O., Olivucci, M., Garavelli, M. Relationship between excited state lifetime and isomerization quantum yield in animal rhodopsins: Beyond the one-dimensional Landau-Zener model. *J. Phys. Chem. Lett.* **2018**, *9*, 3315–3322.
- 23) Kempfer-Robertson, E. M., & Thompson, L. M. Effect of oriented external electric fields on the photo and thermal isomerization of azobenzene. *J. Phys. Chem. A* **2020**, *124*, 18, 3520–3529.
- 24) Bandara, H. M. D., & Burdette S. C. Photoisomerization in different classes of azobenzene. *Chem. Soc. Rev.*, **2012**, *41*, 1809-1825.
- 25) Deshmukh, S. D.; Tsori, Y. Communication: Control of chemical reactions using electric field gradients. *Journal of Chemical Physics* **2016**, *144*.
- 26) García-Amorós, J.; Velasco, D. Recent advances towards azobenzene-based lightdriven real-time information-transmitting materials. *Beilstein Journal of Organic Chemistry* **2012**, *8*, 1003–1017.
- 27) Azuki, M.; Morihashi, K.; Watanabe, T.; Takahashi, O.; Kikuchi, O. Ab initio GB study of the acid-catalyzed cis-trans isomerization of methyl yellow and methyl orange in aqueous solution. *Journal of Molecular Structure: THEOCHEM* **2001**, *542*, 255–262.
- 28) Adalberto Alejo-Molina and Hendradi Hardhienata 2016 *IOP Conf. Ser.: Earth Environ. Sci.* **31** 012020
- 29) Fujino, T.; Arzhantsev, S. Y.; Tahara, T. Femtosecond Time-Resolved Fluorescence Study of Photoisomerization of *trans*-Azobenzene. *J. Phys. Chem. A* **2001**, *105*, 35, 8123–8129.

- 30) Jain, A.; Ramanathan, V.; Sankararamkrishnan, R. Lone pair  $\cdots$   $\pi$  interactions between water oxygens and aromatic residues: Quantum chemical studies based on high-resolution protein structures and model compounds. *Protein Sci.* **2009**, *18*, 3, 595–605.
- 31) Gung, B. W.; Zou, Y.; Xu, Z.; Amicangelo, J. C.; Irwin, D. G.; Ma, S.; Zhou, H. C. Quantitative study of interactions between oxygen lone pair and aromatic rings: substituent effect and the importance of closeness of contact. *J Org Chem.* **2008**, *73*, 2, 689-93.
- 32) Wendler, T.; Schütt, C.; Nather, C.; Herges, R. Photoswitchable Azoheterocycles via Coupling of Lithiated Imidazoles with Benzenediazonium Salts. *J. Org. Chem.* **2012**, *77*, 3284–3287.
- 33) (a) Hohenberg, P.; Kohn, W. Inhomogeneous Electron Gas. *Phys. Rev.*, **1964**, *136*, B864-B71. (b) Kohn, W.; Sham, L. J. Self-Consistent Equations Including Exchange and Correlation Effects. *Phys. Rev.*, **1965**, *140*, A1133-A38. (c) Parr, R. G.; Yang, W. Density-functional theory of atoms and molecules. Oxford Univ. Press, Oxford, **1989**. (d) *The Challenge of d and f Electrons*, Ed. D. R. Salahub and M. C. Zerner (ACS, Washington, D.C., **1989**)
- 34) Frisch, M. J.; Trucks, G. W.; Schlegel, H. B.; Scuseria, G. E.; Robb, M. A.; Cheeseman, J. R.; Scalmani, G.; Barone, V.; Petersson, G. A.; Nakatsuji, H.; Li, X.; Caricato, M.; Marenich, A. V.; Bloino, J.; Janesko, B. G.; Gomperts, R.; Mennucci, B.; Hratchian, H. P.; Ortiz, J. V.; Izmaylov, A. F.; Sonnenberg, J. L.; Williams-Young, D.; Ding, F.; Lipparini, F.; Egidi, F.; Goings, J.; Peng, B.; Petrone, A.; Henderson, T.; Ranasinghe, D.; Zakrzewski, V. G.; Gao, J.; Rega, N.; Zheng, G.; Liang, W.; Hada, M.; Ehara, M.; Toyota, K.; Fukuda, R.; Hasegawa, J.; Ishida, M.; Nakajima, T.; Honda, Y.; Kitao, O.; Nakai, H.; Vreven, T.; Throssell, K.; Montgomery, J. A., Jr.; Peralta, J. E.; Ogliaro, F.; Bearpark, M. J.; Heyd, J. J.; Brothers, E. N.; Kudin, K. N.; Staroverov, V. N.; Keith, T. A.; Kobayashi, R.; Normand, J.; Raghavachari, K.; Rendell, A. P.; Burant, J. C.; Iyengar, S. S.; Tomasi, J.; Cossi, M.; Millam, J. M.; Klene, M.; Adamo, C.; Cammi, R.; Ochterski, J. W.; Martin, R. L.; Morokuma, K.; Farkas, O.; Foresman, J. B.; Fox, D. J. *Gaussian 16*, Revision C.01, Gaussian, Inc., Wallingford CT, 2016.
- 35) Eyring, H. The Activated Complex in Chemical Reactions. *J. Chem. Phys.* **1935**, *3*, 107 –115.
- 36) Grimme, S.; Antony, J.; Ehrlich, S.; Krieg, H. A consistent and accurate ab initio parametrization of density functional dispersion correction (DFT-D) for the 94 elements H-Pu. *J. Chem. Phys.* **2010**, *132*, 154104.
- 37) Dennington, Roy; Keith, Todd A.; Millam, John M. *GaussView*, Version 6, Semichem Inc., Shawnee Mission, KS, 2016.
- 38) Consoli, F.; De Angelis, R.; Robinson, T. S.; Giltrap, S.; Hicks, G. S.; Ditter, E. J.; Ettliger, O. C.; Najmudin, Z.; Notley, M.; Smith, R. A. Generation of intense quasi- electrostatic fields due to deposition of particles accelerated by petawatt-range laser- matter interactions. *Scientific Reports* **2019**, *9*, 1–14.